Functional inertia reveals history-dependent organization of large-scale brain dynamics

Sir-Lord Wiafe[1], Vince D. Calhoun[1]

[1]Tri-Institutional Center for Translational Research in Neuroimaging and Data Science (TReNDS), Georgia State University, Georgia Institute of Technology, and Emory University, Atlanta, GA 30303, USA.

Abstract

Human cognition is deeply contextual: a single moment can reawaken distant memories and emotions, shaping how we perceive and respond through the brain's retention of the past. This continuously reveals an inertial influence, long implicit in brain dynamics, that governs how brain states persist, shift, and reorganize over time. To render this organizing principle observable in neural data, we formalize an inertial state-space model that is agnostic to the observational modality. Applied to resting-state fMRI, we show that functional inertia organizes brain activity into recurrent dynamical regimes, defines a stable whole-brain constraint linked to cognition, and exhibits circuit-level distributions associated with clinical symptoms. In schizophrenia, departures from normative inertial organization emerge consistently across these levels and are mediated by a shared system-level inertial magnitude, resolving apparent contradictions between stability and volatility in brain dynamics reported in prior work. Together, these results position functional inertia as a unifying principle that reframes brain dynamics as history-constrained state evolution rather than transient fluctuations.

Keywords: Functional inertia, Inertia state-space model (ISSM), brain dynamics

1. INTRODUCTION

Biological systems do not respond to the present in isolation. Ongoing behavior emerges from the accumulation of prior states, allowing identical inputs to produce divergent responses depending on historical context[1,2]. In the brain, perception, cognition, and action unfold within this context-dependent landscape, where activity is shaped not only by immediate stimuli but by preceding configurations[3,4]. More broadly, memory-endowed systems evolve under constraints imposed by their past, exhibiting path-dependent dynamics in which present trajectories are conditioned by accumulated history rather than determined solely by instantaneous inputs.

History dependence is not merely an abstract systems-level concept but emerges from concrete neural mechanisms operating across spatial and temporal scales. Recurrent excitation within cortical microcircuits sustains activity patterns, allowing prior configurations to influence processing even in the absence of external input[5,6]. Slow N-methyl-D-aspartate receptor–mediated currents further extend this persistence by integrating synaptic activity over hundreds of milliseconds to seconds, biasing responses toward recent states[1]. At shorter timescales, synaptic facilitation and activity-dependent depression dynamically reshape effective connectivity, such that identical inputs can elicit different outputs depending on preceding activity[7,8]. Neuromodulatory systems, including dopamine, acetylcholine, and norepinephrine, regulate neuronal gain and synaptic efficacy over longer durations, establishing persistent contextual regimes that influence large-scale network dynamics[9-11]. Even in indirect modalities such as fMRI, temporal summation of the blood-oxygenation-level-dependent response introduces additional constraints on apparent state transitions[12]. Together, these multiscale mechanisms render neural processing intrinsically path-dependent, with present responses constrained by accumulated prior states rather than determined solely by instantaneous input.

These observations raise a central question: can we formalize how accumulated context governs the evolution of brain activity, independent of the representations used to describe it? Here, we introduce "*functional inertia"* as an organizing principle reflecting the constraining influence of history on neural reorganization, unifying variability, persistence, and regime structure as expressions of a single constraint on state evolution. To formalize this principle, we develop an inertial state-space model (ISSM) that accumulates observations over time and operationalizes history-conditioned resistance to reconfiguration as an intrinsic property of state evolution (Fig. 1). The framework is observational and scale-agnostic, allowing functional inertia to be instantiated across diverse neural, behavioral, or relational trajectories.

Across spatial and temporal scales, neuroscience provides powerful frameworks for describing brain dynamics, yet state evolution is typically analyzed relative to local configurations or instantaneous variables rather than accumulated history. Microcircuit models track moment-to-moment updates while leaving cumulative trajectories implicit[5,6]. Mesoscopic and electrophysiological approaches characterize evolving patterns but focus on instantaneous configurations rather than contextual constraints[2,13]. At the

macroscopic level, dynamic functional connectivity, hidden Markov models, and meta-state frameworks model transitions among windowed states without treating prior activity as an explicit constraint[14-17]. Even whole-brain generative models specify evolution through instantaneous parameters and structural coupling rather than a formally accumulated governing quantity[18].

The ISSM introduced here directly addresses this gap by formalizing the accumulated context itself as a state variable. Rather than treating observations as isolated configurations, the model recursively integrates them into a running latent trajectory whose evolution reflects the cumulative influence of prior states (Fig. 1). Within this formulation, functional inertia is operationalized by the rate at which this accumulated trajectory changes, providing a quantitative measure of how strongly history constrains present reorganization. Crucially, this framework is agnostic to the form of observation and can be instantiated using spatial activity maps, regional or multivariate time series, relational trajectories such as dynamic connectivity, behavioral sequences, neuromodulatory signals, gene expression profiles, or any temporally evolving biological observable. Although different representations capture distinct aspects of system dynamics, they reflect a shared history-conditioned constraint on state evolution.

We instantiate this general framework using dynamic time warping (DTW) applied to resting-state fMRI. DTW is employed because it accommodates intrinsic timescale variability across regions without assuming strict temporal synchrony, a limitation of many macroscale approaches[19,20]. This also naturally yields a cumulative alignment structure consistent with the temporal integration central to the ISSM[21]. This property makes DTW a particularly informative instantiation of the framework, as it preserves the evolving trajectory of activity that an inertial formulation seeks to characterize. Within this instantiation, functional inertia emerges as a coherent organizing principle expressed at three complementary levels: recurrent whole-brain regimes that characterize modes of state evolution, a stable system-level magnitude linked to cognitive performance and symptom severity, and circuit-specific distributions that differentiate normative and pathological dynamics in schizophrenia. Using schizophrenia as a perturbative case, we show that departures from normative inertial organization manifest consistently across these levels, with regime engagement and circuit-level inertia jointly mediated by a shared system-level inertial magnitude. Under this view, variability, persistence, regime structure, and apparent stability are coordinated expressions of a single history-dependent constraint governing large-scale brain dynamics.

We additionally demonstrate that accumulation of context gives rise to the observed system-level organization and regime-to-whole brain coordination through mediation effects. When the accumulation step alone is removed, these global and mediation-level effects are no longer observed, supporting the premise that cumulative context underlies the organizing principle described here. Moreover, to demonstrate that this organizing principle does not depend on the DTW representational axis, we implement a correlation-based instantiation of the inertial state-space framework, which recovers a comparable hierarchical regime organization and clinically and behaviorally relevant associations. These complementary analyses support functional inertia as a representation-agnostic

organizing principle of brain dynamics, reflecting a property of how accumulated history constrains neural evolution across observational axes.

2. RESULTS

2.1. Recurrent functional inertia states reflect whole-brain dynamical regimes

We introduce an inertial state-space formulation that maps multivariate brain observations to a latent configuration determined by accumulated history. We then introduce the functional inertia index (FII) to quantify how new observations modify this configuration and test whether FII exhibits reproducible dynamical structure and clinically meaningful variation. Functional inertia reflects how resistant the accumulated trajectory is to change. Intuitively, if the latent trajectory is nearly flat, the system is strongly constrained by its past and has high inertia. If the trajectory bends sharply, the system is actively reconfiguring, and inertia is low. We quantify the FII reconfiguration as the rate of change of the accumulated trajectory. Although the formulation is observation-agnostic, here we instantiate it using dynamic time warping applied to interregional time series. Figure 2a illustrates this DTW-based instantiation of the ISSM, in which time-resolved DTW deviations are accumulated to form a latent trajectory and then differentiated to yield the functional inertia index.

We next examine whether the FII exhibits structured dynamical organization over time. We apply k-means clustering to FII values from all interregional pairs and time points, concatenated across subjects, to identify recurrent dynamical states. Across edges, the resulting regimes exhibited strong segregation at the whole-brain level, as shown by the distribution of FII values across interregional pairs within each regime (Fig. 2b). Within a given regime, most edges share the same sign and show a tightly concentrated range of magnitudes. This indicates that, under this instantiation, these functional inertia states are not primarily defined by distinct network configurations but instead reflect global regimes in which the brain collectively resists change or actively reconfigures relative to its past.

We refer to these regimes as locked, stabilizing, and shifting. The locked regime is characterized by FII values near zero and reflects strong resistance to reconfiguration. The stabilizing regime exhibits positive FII values and reflects active reconfiguration toward a more cohesive amplitude configuration, with decreasing interregional disparity. The shifting regime exhibits negative FII values and reflects active reconfiguration toward a more dispersed amplitude configuration, with increasing interregional disparity. These labels are used throughout the remainder of the manuscript. Example whole-brain FII trajectories, obtained by averaging FII across interregional pairs for visualization purposes, illustrate how individuals transition among these regimes over time (Fig. 2c). These findings indicate that brain activity organizes into three recurrent whole-brain

dynamical regimes reflecting varying degrees and directions of resistance to reconfiguration.

2.2. Altered engagement with functional inertia regimes in schizophrenia

If functional inertia reflects an organizing principle of brain dynamics, then disorders characterized by disrupted brain organization, such as schizophrenia, should exhibit systematic alterations in how these regimes are expressed and engaged. Group comparisons reveal significant diagnostic differences in both regime occupancy and persistence (Fig. 3a). Compared with controls, individuals with schizophrenia exhibited higher occupancy and longer persistence in the stabilizing regime, indexed by increased fraction rate (FR) and mean dwell time (MDT) (both $p < 0.01$). Conversely, controls show greater occupancy and persistence in the locked regime, as indexed by higher FR and MDT ($p < 0.05$). No group differences survive correction in transition probabilities.

To further evaluate behavioral relevance, we examine relationships between regime engagement and clinical or cognitive measures. State metrics are significantly associated with symptom severity but not with cognitive performance. Within the schizophrenia group, positive and negative syndrome scale (PANSS) scores are primarily related to altered engagement with the locked and shifting regimes. Higher positive symptom severity is associated with stronger persistence in the locked regime, evidenced by increased self-transition probability, reduced transitions out of the locked regime, and elevated FR and MDT (all $p < 0.05$; Fig. 3b). In parallel, higher positive symptoms are associated with reduced engagement in the shifting regime, including lower self-transition probability and lower FR (both $p < 0.05$). A similar pattern is observed for negative symptoms (Fig. 3c). Higher negative symptom severity is associated with stronger persistence in the locked regime, evidenced by increased self-transition probability and reduced transitions out of the locked regime ($p < 0.01$), as well as higher FR ($p < 0.01$). Negative symptoms are also associated with reduced engagement in the shifting regime, including lower self-transition probability ($p < 0.001$) and reduced FR and MDT ($p < 0.05$).

These results indicate that schizophrenia is characterized by altered engagement of functional inertia regimes. Healthy controls preferentially occupy the locked regime, whereas individuals with schizophrenia show greater engagement of the stabilizing regime. Within the schizophrenia group, symptom severity is specifically linked to prolonged persistence in the locked, high-inertia regime, while greater engagement of shifting dynamics is associated with lower symptom burden. Together, these findings suggest that greater symptom severity is associated with maladaptive persistence in high-inertia states rather than engagement of active reconfiguration dynamics.

2.3. Whole-brain functional inertia index magnitude (FIIM) links regime dynamics to clinical and cognitive variation

Beyond moment-to-moment inertia regime switching, functional inertia may also be expressed as a scan-level, system-level property of brain dynamics. We therefore asked whether the time-averaged strength of functional inertia across the scan relates to symptom severity and cognitive performance. To this end, we examine associations between the time-averaged whole-brain FIIM and clinical and cognitive measures, analyzed separately in individuals with schizophrenia and healthy controls. FIIM is defined as the temporal mean of the absolute functional inertia index, such that lower FIIM reflects stronger overall inertia. Cognitive performance is assessed using the Computerized Multiphasic Interactive Neurocognitive System (CMINDS)[22].

Among individuals with schizophrenia, lower time-averaged FIIM is significantly associated with higher positive and negative symptom severity (Fig. 4a; $p < 0.05$). Because FIIM indexes the overall magnitude of reconfiguration across the scan, this pattern indicates that patients with more severe symptoms exhibit reduced reconfiguration dynamics, consistent with stronger global functional inertia. FIIM is also positively associated with processing speed, such that individuals with higher reconfiguration strength (higher FIIM) show better performance in this domain ($p < 0.05$). In contrast, healthy controls exhibited the opposite relationship between FIIM and cognition (Fig. 4b). In this group, reduced reconfiguration (stronger functional inertia) is associated with better performance across multiple cognitive domains, including processing speed, working memory, verbal and visual learning, reasoning and problem solving, as well as the composite CMINDS score (all $p < 0.05$). Thus, the functional significance of global inertial magnitude differs across diagnostic groups.

Because functional inertia is defined as a cumulative, whole-brain constraint on state evolution, regime engagement captures how this constraint is expressed over time, whereas the time-averaged FIIM quantifies its overall strength. This distinction motivated us to test whether associations between regime engagement and symptom severity are statistically mediated by the time-averaged whole-brain FIIM. Within the schizophrenia group, mediation analyses reveal that time-averaged whole-brain FIIM significantly mediated the relationship between engagement with the locked functional inertia regime and both positive and negative symptom severity (Fig. 5). Greater engagement with the locked regime, indexed by a higher FR and MDT, is associated with lower FIIM, indicating stronger overall functional inertia (path a; $p < 0.01$). In turn, lower FIIM is associated with greater symptom severity after accounting for locked-regime engagement (path b; $p < 0.05$). Importantly, when FIIM is included in the model, the direct associations between locked-regime engagement and symptom severity are no longer significant (path c'), indicating full statistical mediation. Bias-corrected bootstrap tests confirmed significant indirect effects for both positive and negative symptoms, with confidence intervals excluding zero.

To test whether these system-level and mediation-level effects depend specifically on cumulative state integration, we perform an ablation in which the accumulation step is

removed while preserving all other processing components (Supplementary Fig. 4). Although regime segmentation and several group effects remained, whole-brain FIIM associations and mediation effects disappeared without accumulation. These findings indicate that cumulative context is necessary for the emergence of whole-brain inertial organization.

These findings suggest that regime-level dynamics do not operate independently but rather express a shared system-level inertial magnitude. Prolonged engagement in the locked regime predicts symptom severity because it reflects stronger global functional inertia across the scan. The mediation results demonstrate that clinical expression is driven not by regime timing per se, but by the overall magnitude of this cumulative constraint on state evolution. Thus, functional inertia links time-resolved dynamics and stable clinical variation through a single organizing quantity.

2.4. Circuit-level associations of functional inertia index magnitude with cognition and symptoms

While whole-brain analyses establish functional inertia as a system-level property linked to clinical and cognitive variation, they do not reveal how this constraint is distributed across specific circuits. Consequently, we hypothesize that functional inertia should also be selectively embedded within anatomically and functionally meaningful pathways. We therefore localized whole-brain associations by examining relationships between time-averaged FIIM (i.e., time-averaged absolute FII per interregional pair) and cognition and symptom severity across 1,378 interregional brain network pairs. These networks are derived using the NeuroMark template-guided ICA framework optimized for reproducible, standardized network estimation across datasets and disorders[23].

In healthy controls, network-level FIIM shows domain-specific associations with cognitive performance (Fig. 5a). All significant associations show negative coefficients, indicating that lower FIIM (stronger functional inertia) within specific circuits is associated with better cognitive performance. Working memory performance is linked to a focal sensorimotor–visual association pathway, specifically the connection between the postcentral gyrus and the middle occipital gyrus (MOG). Reasoning and problem-solving performance involved a broader set of distributed circuits spanning midline association cortex, frontoparietal control regions, visual association areas, and cerebellar pathways. Prominent connections included couplings between the precuneus and posterior cingulate cortex with occipital regions such as the cuneus and calcarine cortex, as well as anterior cingulate cortex links with middle frontal and middle temporal gyri. Additional associations involved the inferior parietal lobule connections with the visual and sensorimotor cortices and multiple cerebellar couplings with occipital and parietal regions. Collectively, these findings localize normative inertia–cognition relationships to distributed associative integration circuits linking midline default-mode hubs, frontoparietal control regions, visual cortex, and cerebellum.

In schizophrenia, network-level FIIM shows widespread associations with symptom severity. For positive symptoms, 12 interregional connections are significant after FDR correction (Fig. 5b). The majority of these connections (10 edges, 83%) exhibited negative regression coefficients, indicating that stronger functional inertia is associated with greater positive symptom severity. These edges involve midline default-mode regions including the posterior cingulate cortex and precuneus, limbic–thalamo–temporal pathways encompassing the hippocampus and superior temporal gyrus, and fronto-striatal and cerebellar links. The remaining two connections show positive regression coefficients and linked primary somatosensory and visual cortices to higher-order association regions, specifically the posterior cingulate cortex and inferior parietal lobule. Together, these effects converge on distributed default-mode hubs embedded within cortico–striato–thalamo–cerebellar control circuits, while a smaller subset of sensory–association connections suggests that inertia within primary–associative integration pathways may also contribute to positive symptom expression.

For negative symptoms, 29 interregional connections are significantly associated with PANSS-negative scores (Fig. 5b). As observed for positive symptoms, most connections (24 edges, 83%) show negative regression coefficients. These connections spanned midline default-mode regions, including the anterior and posterior cingulate cortex and precuneus, temporal–sensorimotor interactions involving the fusiform and superior temporal gyri coupled with the postcentral gyrus, and occipito-parietal–sensorimotor pathways linking the cuneus and superior parietal lobule with postcentral cortex and cerebellum. The remaining five connections exhibited positive regression coefficients and are concentrated in parietal and occipital association regions, including the bilateral inferior parietal lobule, paracentral lobule, calcarine cortex, and middle occipital gyrus, with links either within these regions or to the anterior cingulate cortex. Notably, the majority of symptom-related associations mirrored the whole-brain effect, such that lower FIIM (stronger inertia) is associated with greater symptom severity. In summary, negative symptoms localize to inertia within midline default-mode hubs embedded in cortico–subcortical control circuits, alongside prominent involvement of sensory–association integration pathways linking parietal, occipital, and sensorimotor regions.

3. DISCUSSION

Brain dynamics are shaped by a persistent constraint imposed by the accumulation of prior states[1,2], which we term functional inertia. Neural activity evolves under this constraint, such that current states reflect how strongly prior configurations shape reorganization. Functional inertia is intrinsic to state evolution and independent of representational scale: it does not describe a particular brain state, but the degree to which any observed configuration resists change. By explicitly characterizing this property, our findings show that stability, structured transitions, and context-dependent persistence arise from an underlying history-dependent organization. Functional inertia,

therefore, provides a unifying perspective on brain dynamics, framing temporal variability as the expression of accumulated history acting on the present.

To quantify this organizing property, we developed an inertial state-space framework that formalizes how observations accumulate to shape latent-state evolution. The formulation is representation-agnostic: different observational axes provide alternative projections of the same constraint rather than distinct mechanisms. Functional inertia can therefore be instantiated using time-resolved brain maps, regional time series, relational profiles, or other temporally evolving biological signals. In the present study, we apply this principle using DTW-based interregional profiles, which accommodate intrinsic timescale variability while preserving the cumulative structure central to the inertial formulation[19].

To further support the representational generality of this organizing principle, we additionally implement a correlation-based instantiation of the inertial state-space model (Supplementary Fig. 3). Despite differences in spatial expression across observational axes, this alternative formulation yields a similar hierarchical low–mid–high inertia organization and preserves meaningful clinical and cognitive associations. This convergence across distinct representational projections indicates that functional inertia does not depend on a particular distance metric or modeling choice but reflects a representation-agnostic constraint on state evolution.

This organizing principle is expressed dynamically through recurrent regimes of state evolution that reflect how strongly the brain resists reconfiguration at any given moment. Intuitively, a system governed by inertia cannot evolve arbitrarily[2]. It will necessarily pass through periods of minimal change, periods of directed movement toward a low-disparity context, and periods of movement away from it. In our data, these dynamics manifest as locked, stabilizing, and shifting regimes. Crucially, these regimes are not distinct spatial states or network configurations, but distinct modes of movement through state space under accumulated history. Their emergence as a three-regime organization reflects a directional inertial structure governing whole-brain evolution rather than isolated changes in connectivity patterns.

Functional inertia clarifies the organization of normative brain dynamics and how departures from this organization arise in schizophrenia. Healthy controls preferentially occupy the locked regime and exhibit greater persistence in this high-inertia state, whereas individuals with schizophrenia show reduced engagement of the locked regime and greater persistence in the stabilizing regime. At face value, this pattern could be misinterpreted as greater “stability” in schizophrenia and greater “rigidity” in controls. However, inertia is inherently contextual. High inertia is adaptive when the system resides within a well-organized, low-disparity latent context, where resistance to reconfiguration preserves a coherent configuration[18]. In contrast, stabilizing dynamics expressed on a

disrupted latent baseline reflect constrained convergence within a limited dynamic range rather than restoration of a well-organized context. Consistent with this interpretation, regime-conditioned analyses show that locked regimes in controls occupy a significantly lower-disparity latent context than stabilizing regimes in schizophrenia, and that all control regimes reside closer to this context than any schizophrenia regime (Supplementary Tables S1 and S3). Thus, stabilizing dynamics in schizophrenia unfold on an already disrupted baseline and do not approach the latent context characteristic of healthy brain dynamics, consistent with prior fMRI and PET evidence of persistent functional disruption[19,24,25]. By separating the direction of reconfiguration from latent-state context, functional inertia provides a principled axis for interpreting why superficially similar dynamical regimes can carry opposite functional meaning. Rather than specifying which configurations occur, this axis constrains how readily the system can depart from established configurations.

When considered in relation to clinical expression, functional inertia suggests that schizophrenia is characterized not by excessive reconfiguration but by prolonged engagement of high-inertia states. Within the schizophrenia group, greater positive and negative symptom severity is associated with prolonged engagement of the locked regime, indicating that when the system enters a high-inertia configuration, it remains there. In this context, high inertia does not reflect adaptive stability but sustained residence within an already disrupted latent configuration. This interpretation aligns with prior dynamic connectivity findings showing that extended residence in weakly integrated or hypoconnected states predicts greater symptom burden[26,27], but extends these observations by demonstrating that symptom severity is most strongly associated with persistence defined at the level of cumulative state evolution rather than instantaneous network patterns. From this perspective, clinical impairment reflects prolonged constraint within maladaptive latent configurations rather than transient fluctuations in connectivity states.

Consistent with the regime-level expression of functional inertia, whole-brain FIIM captures the same organizing principle at a stable, system-level scale with dissociable clinical and cognitive associations. In schizophrenia, stronger overall functional inertia, indicating greater resistance to reconfiguration, is associated with greater positive and negative symptom severity and poorer processing speed[16,27]. In contrast, healthy controls exhibited the opposite pattern: lower FIIM (stronger inertia) is associated with better performance across multiple cognitive domains, including processing speed, working memory, learning, and reasoning[28]. This bidirectional pattern mirrors regime-level findings and suggests that the functional significance of inertia depends on the broader latent context in which it is expressed[18]. In healthy individuals, greater resistance to reconfiguration is associated with better cognitive performance, whereas in

schizophrenia, stronger resistance is associated with greater symptom severity. Thus, the same inertial property appears to carry distinct functional correlates depending on diagnostic context.

Because regime occupancy reflects the temporal expression of functional inertia rather than an independent mechanism, relationships between locked-regime persistence and symptom severity should arise through its overall magnitude. Consistent with this prediction, mediation analyses show that associations between prolonged locked-regime engagement and both positive and negative symptom severity in schizophrenia are accounted for by the time-averaged whole-brain FIIM. Greater locked-regime persistence predicted stronger global inertia, which in turn predicted greater symptom severity, and the direct regime–symptom association is no longer significant once global magnitude is included. These results indicate that regime dynamics and system-level inertia are not independent processes but complementary expressions of a shared constraint on state evolution. Within this framework, relationships between momentary regime engagement and clinical expression reflect how strongly accumulated history imposes global resistance to reconfiguration. Critically, this architecture depended specifically on cumulative state integration. When the accumulation step is removed while preserving DTW alignment, smoothing, and derivatives (Supplementary Fig. 4), whole-brain FIIM associations and mediation effects disappeared. Thus, accumulation is not a redundant preprocessing step but the operation through which local regime dynamics cohere into a global inertial magnitude.

At the circuit level, functional inertia reveals a structured but nonuniform architecture of symptom expression in schizophrenia. Most symptom-related connections show an inverse relationship between inertia and symptom severity, such that lower inertia is associated with lower positive and negative symptoms. These associations are concentrated within distributed associative control hubs embedded within cortico–subcortical integration circuits, including midline default-mode regions such as the posterior cingulate cortex and precuneus, coupled with limbic, thalamo-temporal, fronto-striatal, and cerebellar pathways implicated in hallucinations, delusions, avolition, and social withdrawal[29-33]. This pattern suggests that stronger resistance to reconfiguration within integrative control networks is linked to greater symptom burden, consistent with reports of reduced variability in default-mode and control systems in schizophrenia[26,27]. In contrast, a smaller subset of connections shows the opposite pattern, with lower inertia associated with higher symptom severity, primarily involving sensory–association integration pathways linking primary sensory or sensorimotor cortices with higher-order associative regions. Prior electrophysiological and neuroimaging work indicates that effective sensory integration requires stable coordination between sensory and associative systems, whereas excessive volatility degrades perceptual fidelity and

contextual gating[13,34], consistent with dynamic connectivity findings in schizophrenia[26,35]. Taken together, these findings converge on a dual motif: persistent stability within distributed associative control hubs alongside heightened volatility within sensory–association pathways[27,36,37]. This also aligns with computational models proposing that schizophrenia couples over-stable cortico-cortical scaffolds with noisy thalamo-sensory loops[38,39]. Symptom expression, therefore, appears to reflect the differential distribution of functional inertia across circuits rather than a uniform alteration in reconfiguration capacity.

Several considerations define the scope of the present analyses. Although the inertial state-space formulation is inherently representation-agnostic, and we illustrate this through an additional correlation-based instantiation (Supplementary Fig. 3), the primary analyses focus on a DTW-based formulation applied to resting-state fMRI as a principled example. This choice reflects one concrete instantiation among many possible observational axes rather than a restriction of the framework itself. We further adopt a zero-order instantiation with a uniform cumulative kernel, appropriate for resting-state conditions in which task timing and event structure are unspecified. This assumption does not imply that biological systems weight past experience uniformly; rather, it provides a minimal reference model against which more context-sensitive or adaptive accumulation rules can be evaluated. Extensions to task-evoked paradigms, longitudinal designs, alternative observational representations, and adaptive accumulation kernels would extend the same organizing principle rather than modify its core formulation.

In summary, this work identifies functional inertia as an organizing constraint on brain dynamics and introduces the inertial state-space model as a formal framework for quantifying it through accumulated context. By distinguishing latent-state context from the direction and magnitude of reconfiguration, the formulation clarifies why similar dynamical regimes can carry distinct functional and clinical meaning. Across recurrent regimes, global inertial magnitude, and circuit-level distributions, functional inertia consistently reveals that the significance of brain dynamics depends not only on how activity changes, but on the contextual configuration within which those changes unfold. These findings recast large-scale brain dynamics as history-constrained state evolution, in which cognition and psychopathology emerge from the ongoing interaction between accumulated past configurations and present reorganization. In doing so, functional inertia provides a unified conceptual language for interpreting stability, volatility, and dysfunction in complex brain systems.

4. METHODS

4.1. Inertial state-space formulation of brain dynamics

To formalize the idea that human cognition is shaped by context-dependent accumulation of experience, we adopt an inertial state-space formulation. At an abstract level, this describes how a person's momentary internal state reflects a weighted history of prior states, with past configurations persisting and being differentially expressed depending on the current context. Here, we operationalize this principle using brain data, treating large-scale neural activity as an observable proxy for the underlying cognitive state illustrated schematically in Fig. 1c. The formulation is observational, providing a compact mathematical description of how observations across time contribute to the present latent configuration.

Let $x(t)$ denote the latent state of the system at time t, corresponding to the internal cognitive configuration depicted in the schematic model, and let $y(t)$ denote the observed multivariate brain signal used to infer this state. In its most general continuous-time form, the inertial state-space model is defined as

$$x(t) = \int_0^t B(t, \tau \mid u(t)) y(\tau) d\tau + D(t) u(t), \tag{1}$$

where $B(t, \tau \mid u(t))$ is a context-modulated accumulation kernel specifying how prior observations $y(\tau)$ at time indices $\tau \leq t$ contribute to the current state, and $u(t)$ represents external inputs or contextual influences when present. The term $D(t)u(t)$ captures direct effects of such inputs on the latent state.

Within this formulation, the accumulation kernel defines how present brain states are constructed from observations across time in a context-dependent manner. This captures how state evolution unfolds within a latent space shaped jointly by accumulated history and current context, with functional inertia emerging as the degree to which prior configurations constrain ongoing reorganization.

For discretely sampled neuroimaging data, such as fMRI, the formulation becomes

$$x_t = \sum_{\tau=1}^{t} B(t, \tau \mid u_t) y_\tau + D u_t, \tag{2}$$

where x_t denotes the latent state at time index t, and y_τ the observed signal at time indices $\tau \leq t$. An intuitive version of the ISSM formulation is provided in Fig. 1b.

This formulation is deliberately broad. While we focus here on brain-derived observations, the same inertial description applies to human cognition more generally, with different observational modalities, including neural or behavioral readouts, corresponding to different instantiations of $y(t)$. Different accumulation kernels define alternative operationalizations of inertia, while preserving the principle that present states reflect the cumulative trajectory leading to the present moment.

4.2. Zero-order instantiation of the ISSM

The inertial state-space formulation admits a zeroth-order instantiation in which the latent state is defined solely by accumulated observations, without requiring an explicit, parameterized input or task model. This regime arises naturally when state evolution is driven by internally generated dynamics or by contextual influences that are implicit or unmeasured, as in spontaneous thought, mind-wandering, memory recall, affective drift, or naturalistic conditions such as task-free viewing or listening. In these settings, the absence of explicit inputs does not imply a lack of structure; rather, it isolates a principled limit in which the influence of accumulated history on state evolution can be examined directly.

Resting-state fMRI provides a particularly clear and widely studied example of this regime. In the absence of externally imposed tasks, large-scale brain activity reflects internally generated fluctuations shaped by prior configurations of the system. For discretely sampled zero-order ISSM, we set $u_t = 0$ and equation (2) reduces to

$$x_t = \sum_{\tau=1}^{t} B(t,\tau) y_\tau. \tag{3}$$

A natural and assumption-light choice in this zeroth-order setting is the uniform cumulative kernel,

$$B(t,\tau) = \frac{1}{t}, \qquad 1 \leq \tau \leq t, \tag{4}$$

which yields the ISSM latent representation

$$x_t = \frac{1}{t} \sum_{\tau=1}^{t} y_\tau. \tag{5}$$

This choice does not assert that biological memory is uniform or non-decaying. Rather, it provides a minimal operationalization of inertia by defining the latent state as the running configuration implied by the trajectory to date, such that functional inertia is revealed by the deviation required for new observations to reorganize this configuration. By isolating state evolution from explicit inputs, the zeroth-order instantiation exposes inertia as an intrinsic property of brain dynamics while making the weakest possible assumptions about temporal weighting, task structure, or contextual drives, a choice that aligns naturally with resting-state conditions in which relevant influences are endogenous and unmeasured. More generally, alternative input-free accumulation kernels can be adopted within the same zeroth-order class to reflect different assumptions about temporal integration.

4.3. Functional Inertia and the Functional Inertia Index (FII)

Within the inertial state-space formulation, functional inertia corresponds to resistance to change in the latent state over time. We operationalize this property by quantifying the temporal rate of change of the latent trajectory, which we term the Functional Inertia

Index. Because inertia reflects resistance to change, values of FII close to zero indicate strong inertia, whereas larger-magnitude values indicate active reconfiguration. Formally, the FII at time t is defined as the temporal derivative of the latent state,

$$FII(t) = \frac{d}{dt}x(t), \tag{6}$$

or, in the discrete-time setting,

$$FII_t = x_t - x_{t-1}. \tag{7}$$

This definition holds regardless of how the latent state is constructed and therefore applies across different instantiations of the inertial state-space model.

The sign of the FII provides directional information about state evolution. Depending on the representational axis, positive FII may indicate low-inertia evolution toward a more coherent configuration, whereas negative values indicate low-inertia evolution toward a more divergent configuration. The magnitude of the FII, termed the Functional Inertia Index Magnitude, captures the strength of this deviation irrespective of direction. Importantly, the FII is not a standalone metric but an index derived directly from the inertial state-space formulation. It does not assume specific temporal scales, task structure, or mechanistic forces. Rather, it provides a principled, time-aware quantification of how strongly past configurations constrain present evolution. In this way, the FII serves as an operational lens through which functional inertia, as an organizing property of brain dynamics, can be measured and related to cognition and clinical phenotype.

4.4. Dynamic time warping instantiation of the ISSM

The inertial state-space formulation is agnostic to the representational axis used to define the observed trajectory $y(t)$, as it can be applied to signals ranging from time-varying brain maps and regional activity to connectivity profiles or behavioral measures. Different choices of $y(t)$ thus provide different operational views of the same inertial principle. Here, we instantiate the ISSM using time-resolved interregional profiles that reflect the relational organization of large-scale brain function, in which dynamics emerge from evolving patterns of interaction. In this instantiation, we define the observed trajectory $y(t)$ using dynamic time warping across brain region pairs[20,40].

This choice is motivated by two considerations. First, brain dynamics unfold across multiple and nonuniform timescales, with intrinsic temporal variability that is not well captured by pointwise or fixed-lag comparisons; DTW explicitly accommodates such variability through time-adaptive alignment[21]. Second, DTW yields a distance measure that quantifies the magnitude of deviation between timescale-aligned interregional profiles[21,41]. These distances are non-negative, additive, and are defined as cumulative deformation costs across aligned time points, mirroring the algebraic structure of the accumulative ISSM. In the ISSM, observations are accumulated over time to form a latent trajectory and then differentiated to quantify resistance to reconfiguration; this

accumulate–differentiate pipeline is most naturally interpreted when the observations themselves encode displacement. DTW, therefore, provides a natural operational basis for functional inertia, allowing resistance to change to be expressed as a force-like quantity derived from the cumulative deviation required to rewrite the system's prior configuration.

In the DTW instantiation, the cumulative trajectory reflects interregional amplitude disparity[19]. When this trajectory decreases, disparity is being reduced; when it increases, disparity is growing. The signed FII therefore indicates the direction of reconfiguration (toward reduced versus increased interregional disparity), while its magnitude indicates how strongly the system is reconfiguring. In the DTW instantiation, the derivative of the cumulative disparity trajectory is sign-inverted so that positive FII corresponds to reconfiguration toward reduced interregional disparity and negative FII corresponds to reconfiguration toward increased disparity. The DTW latent trajectory is temporally smoothed before differentiation to reduce high-frequency noise[42]. The full algorithmic details of DTW distance computation, cumulative trajectory construction, parameter selection, and derivative estimation are provided in the Supplementary Methods.

Anchor baseline window: Because the ISSM accumulates observations over time, estimates derived from the earliest frames are inherently unstable and sensitive to transient scanner effects[43]. To ensure a well-defined reference configuration, we define an anchor baseline window at the start of each scan, serving as a stable starting point for cumulative evaluation. This anchor does not imply a shared task or baseline state across individuals; rather, it provides a common reference against which subsequent observations are assessed, allowing us to determine whether new fluctuations reinforce or overcome the running configuration implied by prior activity. All implementation details related to anchor selection are provided in the Supplementary Methods.

4.5. fMRI data & processing

We analyze resting-state fMRI from the Function Biomedical Informatics Research Network (fBIRN) consortium. Data was acquired with a repetition time of 2 s and comprised 160 healthy controls (37.0 ± 10.9 yr, 45 F/115 M) and 151 individuals with schizophrenia (38.8 ± 11.6 yr, 36 F/115 M). Volumes underwent standard preprocessing such as slice-timing correction, rigid-body realignment, MNI spatial normalization, and 6 mm FWHM Gaussian smoothing[44]. Spatially independent components were then extracted using the NeuroMark ICA pipeline[23], yielding 53 intrinsic connectivity networks (ICNs) common to all subjects. The resulting ICN time courses are detrended, despiked, and filtered using a Butterworth bandpass filter with a frequency cutoff of $0.01 - 0.15Hz$[45]. The filter, with an optimal order of 7 as determined by MATLAB's *buttord* function, maintained a passband ripple under $3\ dB$ and a minimum stopband attenuation of $30\ dB$. Finally, we standardize the filtered ICNs through z-score transformation.

4.6. Recurrent functional inertia states estimation

fMRI whole-brain network inertia vectors across brain region pairs are clustered with standard *k*-means because of its widespread use in time-resolved fMRI analysis[27]. Time points across subjects are concatenated into a single time-by-feature matrix (time points as samples, edges as features) prior to k-means clustering. We implement the *k*-means algorithm with cluster numbers ranging from 1 to 10, setting the maximum number of iterations to 10,000 and using 20 random initializations to ensure robust convergence. The city-block (Manhattan) distance metric is selected for its demonstrated robustness in handling high-dimensional data[46]. The optimal cluster number is determined as 3 using the elbow criterion (See Supplementary material).

4.7. State metrics

Using the *k*-means clusters, we characterized each participant's temporal behavior with three metrics. First, the mean dwell time (MDT) measures state persistence by averaging how long a participant remains in a state once it is entered[47]. Second, the fraction rate (FR) reflects overall occupancy by expressing the proportion of the total recording spent in each state[47]. Finally, the state-to-state transition probabilities form the transition matrix (TM), which quantifies the likelihood of a participant moving from one state to any other[47].

4.8. Group analysis & regression models

We assess group differences between healthy controls and individuals with schizophrenia, associations with the Computerized Multiphasic Interactive Neurocognitive System cognitive scores, and associations with the Positive and Negative Syndrome Scale symptom score using generalized linear models (GLM) that included age, sex, scanning site, and mean frame displacement (FD) as covariates. For group difference analyses and CMINDS scores, a normal distribution is assumed, whereas a Poisson distribution is applied for PANSS score associations due to the positive integer and skewed and non-negative integer nature of the fBIRN dataset's PANSS scores[19,48]. Multiple comparisons are controlled with the Benjamini-Hochberg false discovery rate (FDR) procedure.

4.9. Global FIIM & mediation analysis

To characterize whole-brain functional inertia, we summarized the functional inertia index magnitude by averaging it across time for each participant. This global FIIM reflects the overall strength with which past configurations constrain ongoing state evolution throughout the scan, with lower values indicating stronger functional inertia. We test whether the relationship between state-level dynamic metrics and symptom severity is mediated by the global FIIM using a single-mediator framework with covariate adjustment. Statistical significance is evaluated using nonparametric bootstrap resampling. Full mediation model specifications are provided in the Supplementary Methods.

5. ACKNOWLEDGMENT

This work was supported by the National Institutes of Health (NIH) grant (R01MH123610) and the National Science Foundation (NSF) grant #2112455.

6. DECLARATION OF COMPETING INTEREST

None.

7. DATA & CODE AVAILABILITY STATEMENT

The codes for all our analyses in MATLAB can be accessed through GitHub. The data was not collected by us and was provided in a deidentified manner. The IRB will not allow the sharing of data or individual derivatives, as a data reuse agreement was not signed by the subjects during the original acquisition.

8. REFERENCES

1. Buonomano DV, Maass W. State-dependent computations: spatiotemporal processing in cortical networks. *Nature Reviews Neuroscience.* 2009;10(2):113-125.
2. Kelso JA. Multistability and metastability: understanding dynamic coordination in the brain. *Philos Trans R Soc Lond B Biol Sci.* 2012;367(1591):906-918.
3. Mante V, Sussillo D, Shenoy KV, Newsome WT. Context-dependent computation by recurrent dynamics in prefrontal cortex. *Nature.* 2013;503(7474):78-84.
4. Churchland MM, Cunningham JP, Kaufman MT, et al. Neural population dynamics during reaching. *Nature.* 2012;487(7405):51-56.
5. Wang XJ. Synaptic reverberation underlying mnemonic persistent activity. *Trends Neurosci.* 2001;24(8):455-463.
6. Major G, Tank D. Persistent neural activity: prevalence and mechanisms. *Curr Opin Neurobiol.* 2004;14(6):675-684.
7. Abbott LF, Varela JA, Sen K, Nelson SB. Synaptic depression and cortical gain control. *Science.* 1997;275(5297):220-224.
8. Zucker RS, Regehr WG. Short-term synaptic plasticity. *Annu Rev Physiol.* 2002;64:355-405.
9. Seamans JK, Yang CR. The principal features and mechanisms of dopamine modulation in the prefrontal cortex. *Progress in Neurobiology.* 2004;74(1):1-58.
10. Decker AL, Duncan K. Acetylcholine and the complex interdependence of memory and attention. *Current Opinion in Behavioral Sciences.* 2020;32:21-28.
11. Bouret S, Sara SJ. Network reset: a simplified overarching theory of locus coeruleus noradrenaline function. *Trends in Neurosciences.* 2005;28(11):574-582.
12. Logothetis NK, Pauls J, Augath M, Trinath T, Oeltermann A. Neurophysiological investigation of the basis of the fMRI signal. *nature.* 2001;412(6843):150-157.
13. Varela F, Lachaux J-P, Rodriguez E, Martinerie J. The brainweb: Phase synchronization and large-scale integration. *Nature Reviews Neuroscience.* 2001;2(4):229-239.
14. Allen EA, Damaraju E, Plis SM, Erhardt EB, Eichele T, Calhoun VD. Tracking whole-brain connectivity dynamics in the resting state. *Cereb Cortex.* 2014;24(3):663-676.
15. Baker AP, Brookes MJ, Rezek IA, et al. Fast transient networks in spontaneous human brain activity. *eLife.* 2014;3:e01867.

16. Miller RL, Yaesoubi M, Turner JA, et al. Higher Dimensional Meta-State Analysis Reveals Reduced Resting fMRI Connectivity Dynamism in Schizophrenia Patients. *PLoS One.* 2016;11(3):e0149849.
17. Wiafe S-L, Soleimani N, Calhoun VD. Dynamic Co-Modulation (DyCoM): A Unified Operator Framework for Dynamic Connectivity in Neuroimaging. *bioRxiv.* 2026:2026.2001.2022.701132.
18. Deco G, Tononi G, Boly M, Kringelbach ML. Rethinking segregation and integration: contributions of whole-brain modelling. *Nature Reviews Neuroscience.* 2015;16(7):430-439.
19. Wiafe S-L, Kinsey S, Soleimani N, et al. Aberrant Recovery of Timescale-Aligned Amplitude Balance Links to Symptoms and Cognition in Schizophrenia. *bioRxiv.* 2025:2025.2003.2020.644399.
20. Wiafe S-L, Faghiri A, Fu Z, Miller R, Preda A, Calhoun VD. The dynamics of dynamic time warping in fMRI data: a method to capture inter-network stretching and shrinking via warp elasticity. *Imaging Neuroscience.* 2024;2:1-23.
21. Sakoe H, Chiba S. Dynamic programming algorithm optimization for spoken word recognition. *IEEE transactions on acoustics, speech, and signal processing.* 2003;26(1):43-49.
22. O'Halloran JP, Kemp AS, Gooch KN, et al. Psychometric comparison of computerized and standard administration of the neurocognitive assessment instruments selected by the CATIE and MATRICS consortia among patients with schizophrenia. *Schizophrenia Research.* 2008;106(1):33-41.
23. Du Y, Fu Z, Sui J, et al. NeuroMark: An automated and adaptive ICA based pipeline to identify reproducible fMRI markers of brain disorders. *Neuroimage Clin.* 2020;28:102375.
24. Dwyer DS, Bradley RJ, Kablinger AS, Freeman AM, 3rd. Glucose metabolism in relation to schizophrenia and antipsychotic drug treatment. *Ann Clin Psychiatry.* 2001;13(2):103-113.
25. Newcomer JW, Haupt DW, Fucetola R, et al. Abnormalities in glucose regulation during antipsychotic treatment of schizophrenia. *Arch Gen Psychiatry.* 2002;59(4):337-345.
26. You W, Luo L, Yao L, et al. Impaired dynamic functional brain properties and their relationship to symptoms in never treated first-episode patients with schizophrenia. *Schizophrenia.* 2022;8(1):90.
27. Damaraju E, Allen EA, Belger A, et al. Dynamic functional connectivity analysis reveals transient states of dysconnectivity in schizophrenia. *Neuroimage Clin.* 2014;5:298-308.
28. Garrett DD, Kovacevic N, McIntosh AR, Grady CL. The Importance of Being Variable. *The Journal of Neuroscience.* 2011;31(12):4496-4503.
29. Forlim CG, Klock L, Gallinat J, Kühn S. Altered resting-state functional connectivity in a thalamo-cortico-cerebellar network in patients with schizophrenia. *Sci Rep.* 2024;14(1):26284.
30. Bernard JA, Orr JM, Mittal VA. Cerebello-thalamo-cortical networks predict positive symptom progression in individuals at ultra-high risk for psychosis. *Neuroimage Clin.* 2017;14:622-628.
31. Opjordsmoen S. Delusional Disorder as a Partial Psychosis. *Schizophrenia Bulletin.* 2014;40(2):244-247.
32. Manoliu A, Riedl V, Doll A, et al. Insular Dysfunction Reflects Altered Between-Network Connectivity and Severity of Negative Symptoms in Schizophrenia during Psychotic Remission. *Frontiers in Human Neuroscience.* 2013;Volume 7 - 2013.

33. Moessnang C, Otto K, Bilek E, et al. Differential responses of the dorsomedial prefrontal cortex and right posterior superior temporal sulcus to spontaneous mentalizing. *Hum Brain Mapp.* 2017;38(8):3791-3803.
34. Zhou G, Lane G, Noto T, et al. Human olfactory-auditory integration requires phase synchrony between sensory cortices. *Nature Communications.* 2019;10(1):1168.
35. Dong D, Duan M, Wang Y, et al. Reconfiguration of Dynamic Functional Connectivity in Sensory and Perceptual System in Schizophrenia. *Cerebral Cortex.* 2018;29(8):3577-3589.
36. Demirtaş M, Tornador C, Falcón C, et al. Dynamic functional connectivity reveals altered variability in functional connectivity among patients with major depressive disorder. *Hum Brain Mapp.* 2016;37(8):2918-2930.
37. Woodward ND, Karbasforoushan H, Heckers S. Thalamocortical dysconnectivity in schizophrenia. *Am J Psychiatry.* 2012;169(10):1092-1099.
38. Uhlhaas PJ, Singer W. Abnormal neural oscillations and synchrony in schizophrenia. *Nature Reviews Neuroscience.* 2010;11(2):100-113.
39. Rolls ET, Deco G. A computational neuroscience approach to schizophrenia and its onset. *Neurosci Biobehav Rev.* 2011;35(8):1644-1653.
40. Meszlényi RJ, Hermann P, Buza K, Gál V, Vidnyánszky Z. Resting state fMRI functional connectivity analysis using dynamic time warping. *Frontiers in neuroscience.* 2017;11:75.
41. Wiafe S-L, Calhoun VD. Warp Quantification Analysis: A Framework For Path-based Signal Alignment Metrics. *arXiv preprint arXiv:250914994.* 2025.
42. Oppenheim AV. *Discrete-time signal processing.* Pearson Education India; 1999.
43. Power JD, Plitt M, Laumann TO, Martin A. Sources and implications of whole-brain fMRI signals in humans. *Neuroimage.* 2017;146:609-625.
44. Penny WD, Friston KJ, Ashburner JT, Kiebel SJ, Nichols TE. *Statistical parametric mapping: the analysis of functional brain images.* Elsevier; 2011.
45. Yaesoubi M, Allen EA, Miller RL, Calhoun VD. Dynamic coherence analysis of resting fMRI data to jointly capture state-based phase, frequency, and time-domain information. *Neuroimage.* 2015;120:133-142.
46. Aggarwal CC, Hinneburg A, Keim DA. On the surprising behavior of distance metrics in high dimensional space. Paper presented at: Database Theory—ICDT 2001: 8th International Conference London, UK, January 4–6, 2001 Proceedings 82001.
47. Iraji A, Faghiri A, Lewis N, Fu Z, Rachakonda S, Calhoun VD. Tools of the trade: estimating time-varying connectivity patterns from fMRI data. *Social Cognitive and Affective Neuroscience.* 2020;16(8):849-874.
48. Santoro ML, Ota V, de Jong S, et al. Polygenic risk score analyses of symptoms and treatment response in an antipsychotic-naive first episode of psychosis cohort. *Transl Psychiatry.* 2018;8(1):174.

9. FIGURES

Fig. 1: Functional inertia as a history-dependent constraint on brain state evolution.

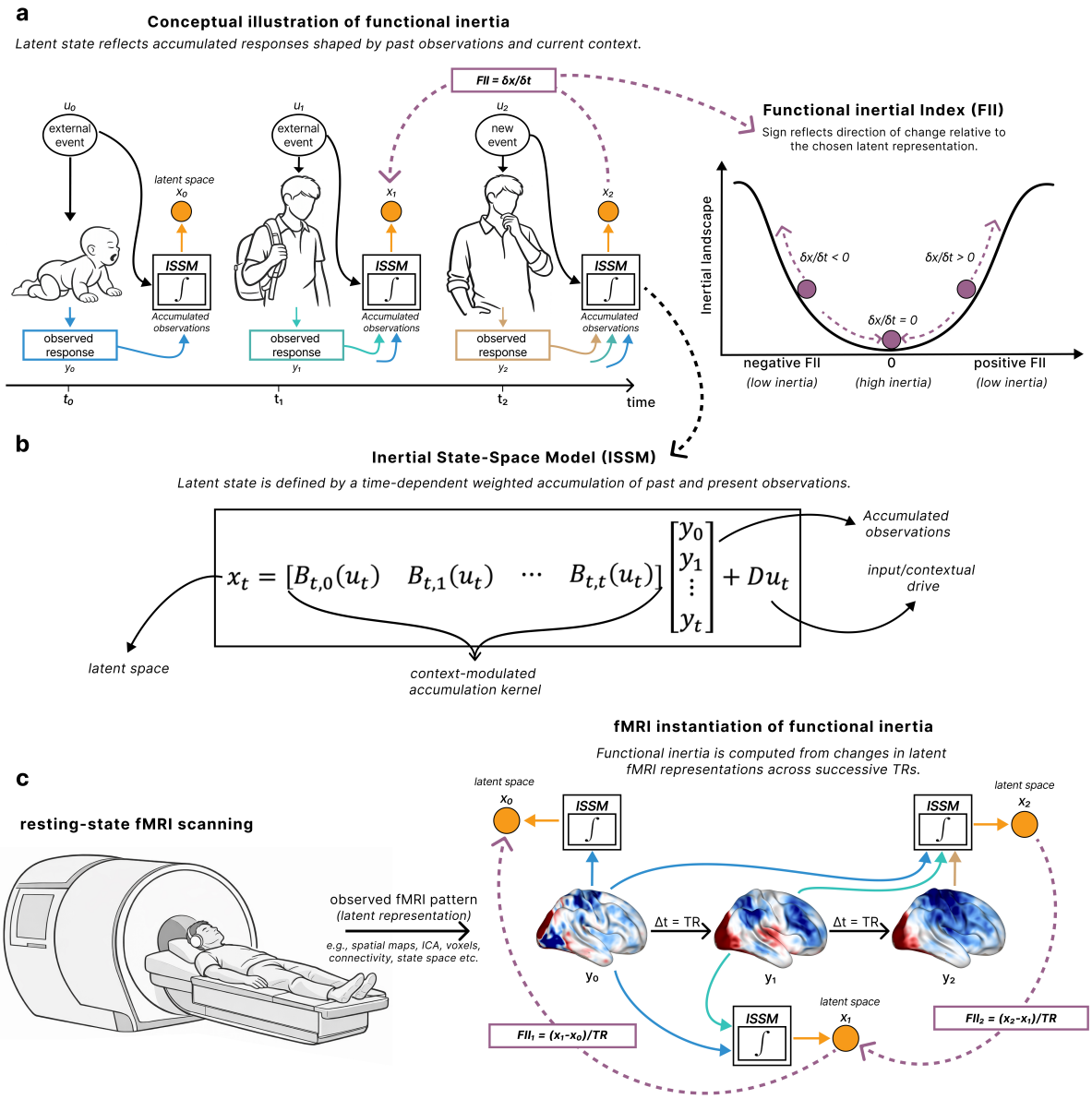

(a) Conceptual illustration of functional inertia. Responses observed at successive time points are accumulated into a latent state that reflects the system's prior trajectory and current context. These observations may reflect neural, behavioral, or physiological signals. Functional inertia is quantified as the temporal rate of change of the latent state, such that values near zero indicate strong resistance to reconfiguration, whereas nonzero values reflect active reorganization relative to accumulated history. (b) Inertial state-space model (ISSM). The latent state x_t is defined as a context-modulated accumulation of past observations y_τ through an accumulation kernel $B(t,\tau)$, with optional external inputs u_t. This formulation is observational and independent of the representational modality used to describe system dynamics. (c) One instantiation of functional inertia in resting-state fMRI. fMRI observations are mapped to latent representations across successive repetition times, and changes in the accumulated latent trajectory are used to compute the functional inertia index. While illustrated here using fMRI, the framework generalizes naturally to other observational modalities through alternative definitions of the observed trajectory $y(t)$.

Fig. 2: Dynamic time warping instantiation of functional inertia and emergent dynamical regimes

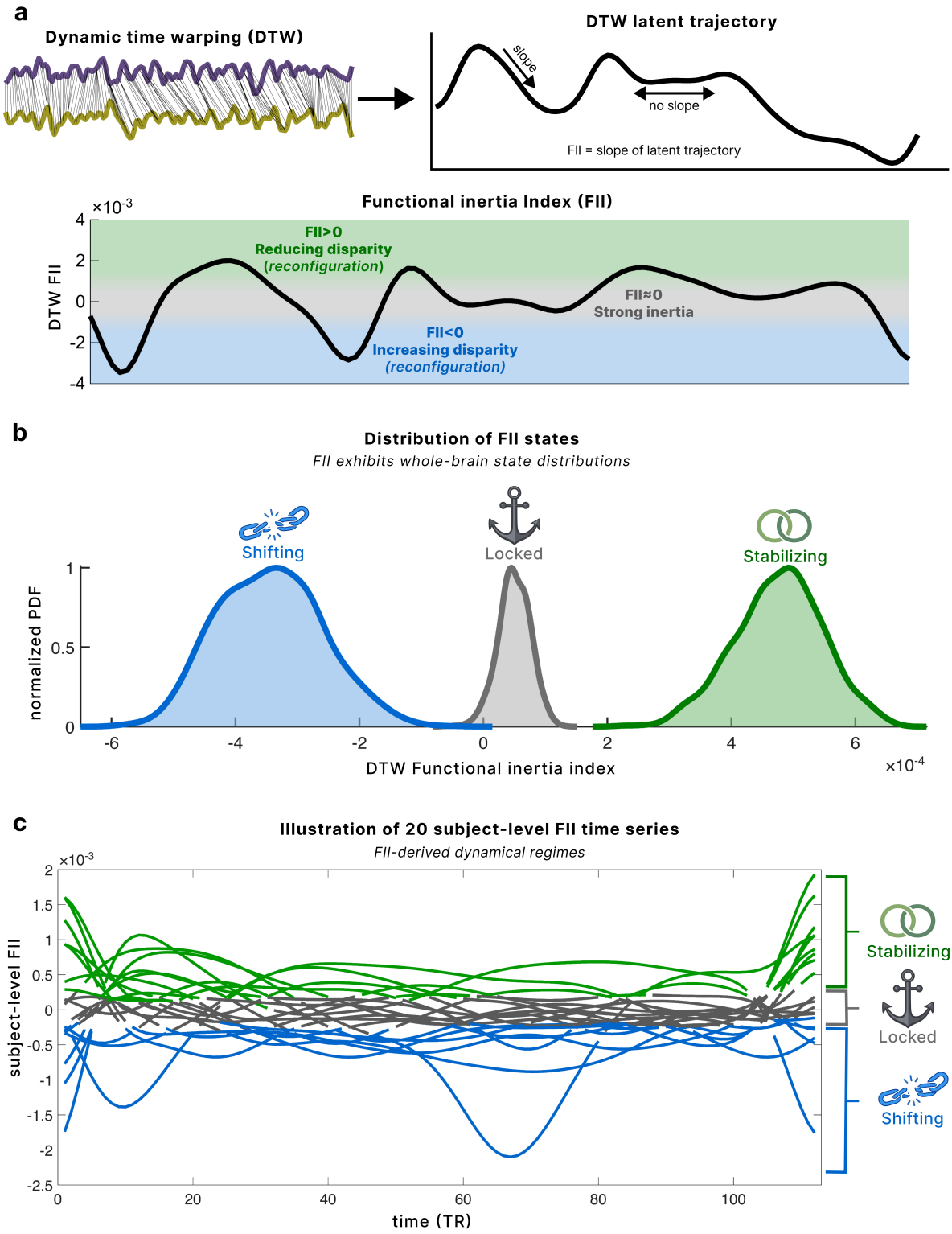

(a) *Dynamic time warping (DTW) aligns interregional amplitude trajectories while accommodating intrinsic timescale variability, yielding a time-resolved deviation signal. This deviation is recursively accumulated to form a latent trajectory that reflects the integrated history of prior observations. The functional inertia index (FII) is defined as the temporal rate of change of this accumulated trajectory. Values near zero indicate strong inertia, where the latent configuration strongly constrains current activity, whereas larger positive or negative values reflect active reconfiguration of the accumulated state.* ***(b)*** *Distribution of functional inertia states across the whole brain. Pooling FII values across all subjects, time points, and interregional pairs reveals a trimodal distribution corresponding to three distinct dynamical regimes. These regimes are centered around negative FII values (shifting), near-zero FII values (locked), and positive FII values (stabilizing), indicating that functional inertia organizes brain dynamics into qualitatively distinct modes of state evolution.* ***(c)*** *Subject-level functional inertia time series illustrating recurrent dynamical regimes. Representative FII trajectories from 20 individuals show that these regimes recur over time within individuals and are expressed coherently across interregional pairs. Shifting, locked, and stabilizing regimes reflect whole-brain dynamical states defined by how the system moves through its latent space under the constraint of accumulated history, rather than by specific spatial network configurations.*

Fig. 3: Engagement with functional inertia regimes across health and disorder

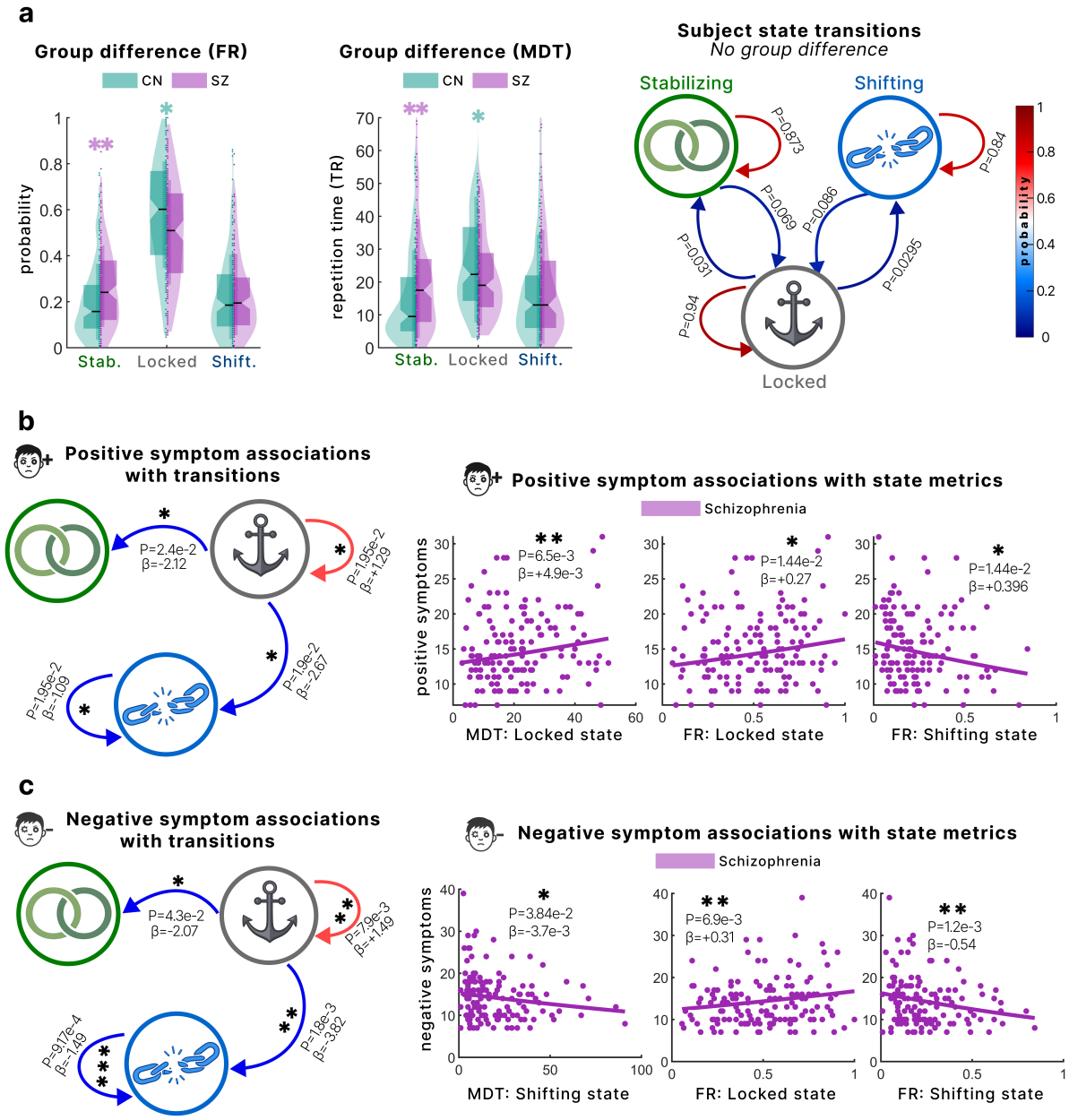

(a) *Group differences in functional inertia regime engagement and transition structure. Left and middle panels show group comparisons between healthy controls (CN) and individuals with schizophrenia (SZ) for fraction rate (FR) and mean dwell time (MDT) across stabilizing, locked, and shifting regimes. Individuals with schizophrenia exhibit increased occupancy and persistence in the stabilizing regime and reduced engagement of the locked regime, whereas no significant group differences are observed in state transition probabilities (right), indicating preserved transition structure but altered regime expression.* ***(b)*** *Associations between positive symptom severity and functional inertia dynamics in schizophrenia. Left, state-transition associations show that higher positive symptom severity is linked to reduced transitions out of the locked regime and reduced engagement of the shifting regime. Right, regression analyses demonstrate that greater persistence (MDT) and occupancy (FR) of the locked regime are associated with higher positive symptom severity, while greater engagement of the shifting regime is associated with lower symptom severity.* ***(c)*** *Associations between negative symptom severity and functional inertia dynamics in schizophrenia. Left, transition analyses reveal that higher negative symptom severity is associated with increased self-persistence of the locked regime and reduced transitions involving the shifting regime. Right, higher negative symptom severity is associated with increased occupancy of the locked regime and reduced engagement of the shifting regime. Together, these results indicate that symptom severity is linked to prolonged expression of high-inertia states and reduced access to low-inertia reconfiguration dynamics.*

Fig. 4: Whole-brain functional inertia magnitude differentially relates to cognition and symptoms across health and disorder

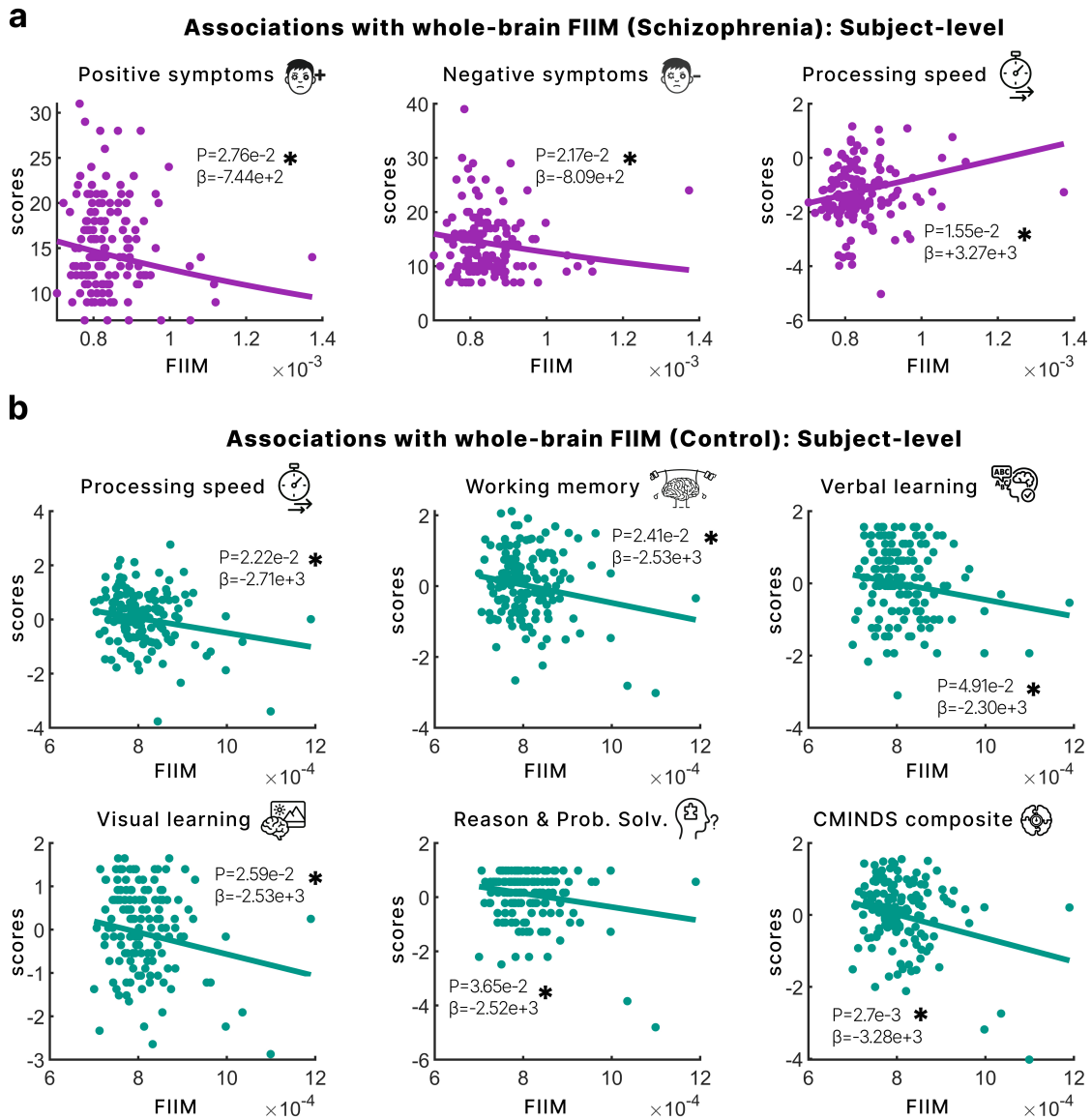

(a) *Associations between whole-brain Functional Inertia Index Magnitude (FIIM) and clinical and cognitive measures in individuals with schizophrenia. Lower FIIM, reflecting stronger overall functional inertia expressed across time and interregional pairs, is associated with greater positive and negative symptom severity and with poorer processing speed. Each point represents a subject; lines indicate fitted regression relationships after covariate adjustment.* ***(b)*** *Associations between whole-brain FIIM and cognitive performance in healthy controls. In contrast to schizophrenia, stronger functional inertia (lower FIIM) is associated with better performance across multiple cognitive domains, including processing speed, working memory, verbal learning, visual learning, reasoning and problem solving, and the composite CMINDS score. Together, these results show that functional inertia is expressed as a stable, system-level property of brain dynamics with dissociable functional consequences depending on the underlying latent-state context.*

Fig. 5: System-level functional inertia mediates the relationship between inertia regime engagement and symptom severity

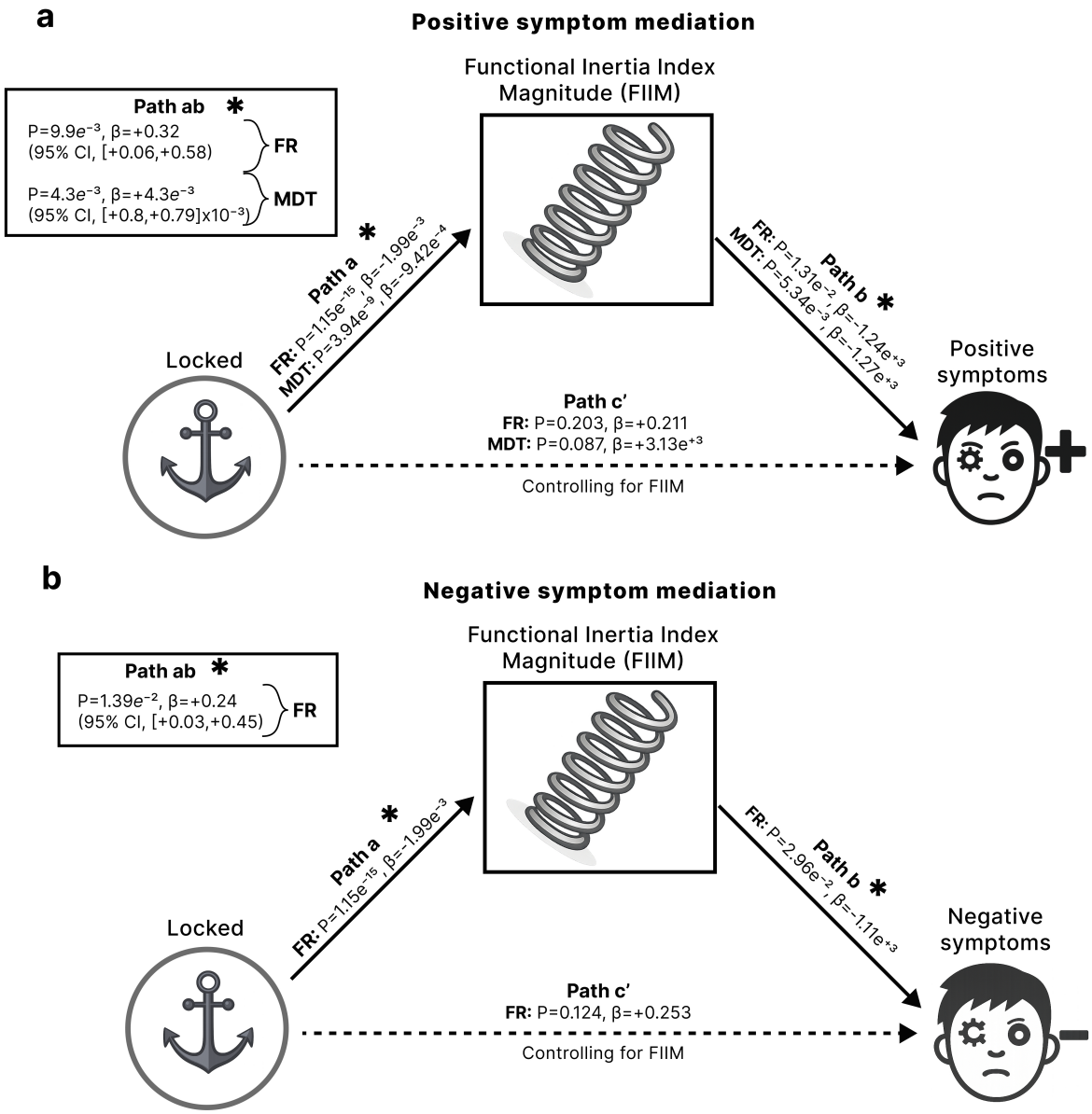

(a) *Mediation analysis for positive symptom severity in schizophrenia. Greater engagement of the locked functional inertia regime, quantified by fraction rate (FR) and mean dwell time (MDT), predicts stronger whole-brain Functional Inertia Index Magnitude (FIIM) (path a). Stronger functional inertia, in turn, predicts greater positive symptom severity (path b). When controlling for FIIM, the direct association between locked-regime engagement and positive symptoms is no longer significant (path c′), indicating full statistical mediation.* ***(b)*** *Mediation analysis for negative symptom severity. Engagement of the locked regime, indexed by FR, is associated with whole-brain FIIM (path a), which in turn predicts negative symptom severity (path b). As in the positive symptom model, the direct association between locked-regime engagement and symptoms is attenuated after accounting for FIIM (path c′), supporting mediation by a shared system-level inertial magnitude. These analyses demonstrate that symptom expression is not driven by regime timing alone but is mediated by the overall strength of functional inertia expressed across the brain.*

Fig. 6: Circuit-level distribution of functional inertia links cognition and symptoms

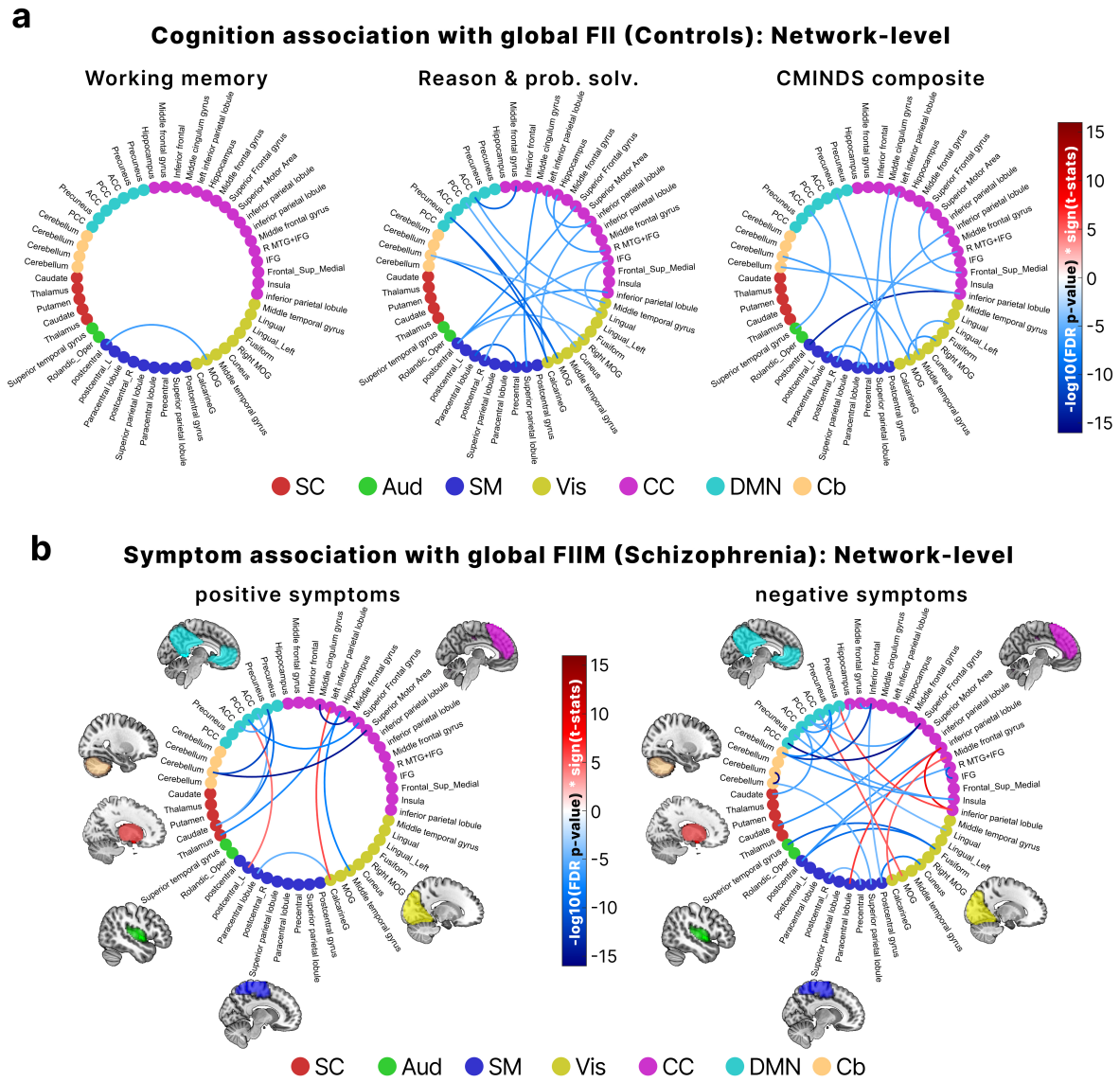

(a) *Network-level associations between time-averaged whole-brain Functional Inertia Index Magnitude (FIIM) and cognitive performance in healthy controls. Significant associations are shown for working memory, reasoning and problem solving, and the CMINDS composite score. Edges indicate interregional connections whose FIIM significantly relates to cognitive performance after FDR correction, colored by the direction and strength of association (signed* $-log_{10}$ *FDR-corrected p-values). Node colors indicate large-scale functional systems, including subcortical (SC), auditory (Aud), sensorimotor (SM), visual (Vis), cognitive control (CC), default mode (DMN), and cerebellar (Cb) networks. Stronger functional inertia within distributed association, midline, and cerebellar circuits is associated with better cognitive performance.* ***(b)*** *Network-level associations between FIIM and clinical symptom severity in schizophrenia. Connections whose FIIM significantly relates to positive (left) and negative (right) symptom severity are shown. Most symptom-related associations involve midline default-mode hubs, limbic–thalamo–temporal pathways, fronto-striatal, cerebellar, and temporal–sensorimotor circuits, with stronger functional inertia predicting greater symptom severity in most connections. A smaller subset of sensory–association couplings exhibits the opposite relationship. These results demonstrate that functional inertia is differentially distributed across circuits and that its cognitive and clinical relevance depends on where resistance to reconfiguration is expressed within the brain.*